Inherent lifetime widths of Ar $2p^{-1}$, Kr $3d^{-1}$, Xe $3d^{-1}$, and Xe $4d^{-1}$ states

M. Jurvansuu, A. Kivimäki, and S. Aksela
Department of Physical Sciences, P.O. Box 3000, FIN-90014 University of Oulu, Finland
(Received 6 March 2001; published 5 June 2001)

The natural widths of the Ar $2p^{-1}$, Kr $3d^{-1}$, Xe $3d^{-1}$, and Xe $4d^{-1}$ states have been determined from photoelectron spectra measured with very high resolution. Lifetime widths Γ_L of 104 ± 3 meV and 111 ± 3 meV were obtained for the Xe $4d_{3/2}^{-1}$ and $4d_{5/2}^{-1}$ states, respectively. In contrast, no differences in the inherent lifetime width could be found for the spin-orbit split components of Ar $2p$ ($\Gamma_L=118\pm4$ meV) and Kr $3d$ ($\Gamma_L=88\pm4$ meV) ionized states. The lifetime widths of the Xe $3d_{3/2}^{-1}$ and $3d_{5/2}^{-1}$ states were found to be 490 ± 30 meV and 510 ± 30 meV, respectively. The extracted lifetime widths are compared with the previously published experimental results.

DOI: 10.1103/PhysRevA.64.012502 PACS number(s): 32.70.Jz, 32.80.Fb

I. INTRODUCTION

When a certain amount of energy is introduced to an atom (or to a molecule), it can be lifted to a higher-energy state. Such an excited state can decay to lower-energy states via radiative (fluorescence) or nonradiative (Auger or autoionizing) transitions. Each of the possible decay channels has a particular transition probability. The lifetime of the excited state is proportional to the inverse of the sum of all partial transition probabilities. The Heisenberg uncertainty principle states that the finite lifetime of the excited state leads to a finite uncertainty in the energy of the excited state. The excited state has a Lorentzian energy distribution, the full width at half maximum (FWHM) of which gives the lifetime width of the state in question [1].

A straightforward way to obtain the lifetime width of a singly ionized state is to measure the corresponding photoelectron spectrum. The total experimental width of the photoelectron line consists of contributions from the inherent Lorentzian lifetime width, photon bandwidth, Doppler broadening due to the thermal motion of the atoms and the finite resolution of the kinetic energy analyzer. More precisely, the observed line profile is the convolution of the partial profiles describing separately each of the above-mentioned broadening source. For the accurate determination of the lifetime width one should have both a narrow photon bandwidth and good analyzer resolution compared to the lifetime width. Recent developments in synchrotron-radiation sources, monochromators, and electron spectrometers are nowadays providing excellent means for such studies.

The model of the two-step process of Auger and radiative decay gives another possibility to determine the core-hole lifetime widths. In this context photoionization and subsequent decay are considered as separate processes; the core-hole state after photoionization is the initial state of the following decay. Some of the final states are long lived and therefore have very narrow-lifetime widths. The energy distributions of the emitted Auger electrons and fluorescent photons carry then detailed information about the lifetime width of the initial state.

The measurements of photoabsorption resonances below the threshold also allow to estimate the lifetime widths of core-ionized states. This is based on the assumption that the electron excited to the Rydberg orbital does not appreciably change the total transition rate of the core-hole state. This condition is best fulfilled when the excited electrons reside on the highest Rydberg orbitals. In this method, the total absorption of the photons is measured as a function of the photon energy after light has passed through the studied gas. More often, the measurement is done by measuring the total electron or ion yield while scanning the photon energy. The lifetime widths of the core-excited states can be obtained also by using the electron-energy loss spectroscopy [2,3]. The tunable narrow-band synchrotron radiation has recently provided rather accurate-lifetime widths for the core-excited states of noble gases and simple molecules [4–7].

In this paper, we determine the lifetime widths of the Ar $2p^{-1}$, Kr $3d^{-1}$, Xe $3d^{-1}$, and Xe $4d^{-1}$ states using high-resolution photoelectron spectroscopy. The Ar $2p$ lifetime widths were determined to be 120 meV by x-ray emission spectroscopy by Nordgren *et al.* [8]. Recently, Carroll *et al.* [9] extracted the same result from the Ar $2p_{3/2}$ photoelectron line. Slightly different values were reported in Refs. [10,11]. The lifetime widths appear not to have been determined for the Kr $3d^{-1}$ states with any high accuracy. Their widths are commonly assumed to be the same as those of the core-excited $3d^{-1}5p$ states (83 meV [2,4]). For Xe $4d^{-1}$ states, the lifetime widths recently reported in literature vary from 110 meV to 121 meV [12–14]. Ausmees *et al.* [12] found evidence on the photon energy dependence of the Xe $4d$ lifetime widths close to the $4d$ threshold. The lifetime width of the Xe $3d^{-1}$ states was estimated to be 0.5 eV from the photoelectron spectra by Svensson *et al.* [15] and by Bancroft *et al.* [16] using monochromatized Al $K\alpha$ x-ray radiation.

II. EXPERIMENT

The photoelectron spectra were measured on the gas phase beam line I411 [17] at the third-generation storage ring MAX-II, Lund, Sweden. The synchrotron radiation is produced by a hybrid undulator in the photon energy range from 50 to 1500 eV. The degree of linear polarization of light is better than 98%, as determined using the Xe $5s$ photoelectron line together with Xe $N_{4,5}O_{2,3}O_{2,3}$ Auger spectrum. Ra-

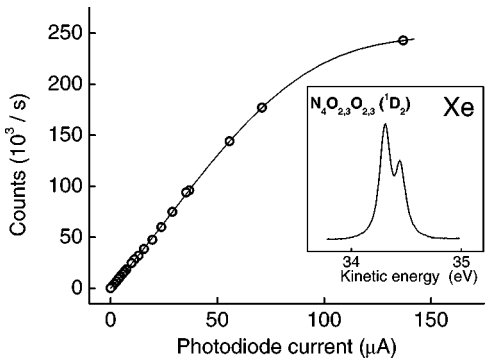

FIG. 1. The intensity of Xe $N_4O_{2,3}O_{2,3}(^1D_2)$ Auger line as a function of the photodiode current. The plot shows observed count rate in the microchannel plate of the SES-200 electron spectrometer. The black-and-white detection mode was used at the measurements. Line is drawn through the measured points to guide the eye.

diation from the undulator is monochromatized by a modified SX-700 plane-grating monochromator [18,19] equipped with a plane elliptical focusing mirror. After the monochromator exit slit, light is refocused by a toroidal mirror. The differential pumping stage separates the low-vacuum ($\sim 10^{-6}$ mbar) gas phase side from the rest of the beam line. The end station [20] is equipped with a high-resolution Scienta SES–200 electron analyser [21]. Electrons are detected with a position-sensitive multichannel plate detector. The analyzer is rotatable around the photon beam between the 0°–90°.

The electron spectra were collected with the SES-200 analyzer at the so-called ''magic'' angle of 54.7° with respect to the electric vector of the photon beam. The analyzer pass energy was set at 10 eV, monochromator exit slit was 10 μm and kept constant during the measurements. Pressure in the analyzer chamber was typically 3×10^{-7} mbar during the measurements that corresponds to the pressure approximately 10^2–10^3 times higher in the gas cell. The low gas pressure was chosen to reduce plasma potentials [22] inside the gas cell. The plasma potentials can cause line broadening mainly by shifting the kinetic energy of the photoelectron line between separate scans.

The saturation of the detector can also lead to line broadening. This is because at the top of the peak the count rate is highest, but due to the saturation, all counts are not recorded. In the line shape, this is seen as a flattening of the peak and correspondingly, the FWHM of the peak increases. To find the saturation point, we measured the intensity of the Xe $N_4O_{2,3}O_{2,3}(^1D_2)$ Auger line as a function of the photon intensity (see Fig. 1). The photon flux was varied by adjusting the monochromator exit slit and the photodiode current was recorded together with the Auger line maximum intensity (not the peak area). The spectra were measured in the pulse counting or black-and-white mode and the time for each energy channel set at 0.2 s. From the individual spectra, we found that a clear saturation occurs with count rates higher than 100 000 counts/s, but for very high resolution work, the count rate should be limited below 50 000 counts/s with the current detector.

III. EXPERIMENTAL BROADENINGS

The Kr $4p_{3/2}$ photoelectron line was measured over the kinetic energy range 41–107 eV to determine the analyzer contribution to the total linewidth. Corresponding to ionization from the outermost shell, the $4p_{3/2}^{-1}$ state has a negligible inherent lifetime width and the experimental line broadening consist only from photon bandwidth, analyzer resolution, Doppler broadening and possible plasma and surface potentials. All these contributions are considered to be Gaussians. This assumption was found to be rather good by fitting the measured Kr $4p_{3/2}$ photoelectron spectra. They showed almost perfect Gaussian shapes, only distorted slightly on the tail where the count rate was below 3% of that of the peak maximum. It should be noticed that the main contribution to the total linewidth comes from the analyzer resolution at these low photon energies. At higher photon energies, such as used for Xe $3d$ ionization (ionization limits: $3d_{3/2}$ $=676.4$ eV, $3d_{5/2}=689.0$ eV [23]), the photon bandwidth gives the largest contribution to the linewidth and the observed line shape may differ more from a Gaussian. However, in our earlier measurements [24] at photon energies $\sim$870 eV, the Ne $2s$ photoelectron line showed only slight asymmetry in the observed line shape. Because the monochromator bandwidth $\Gamma_{h\nu}$ behaves as $\propto E(h\nu)^{3/2}$ [25], the peak asymmetry probably decreases at photon energies used in the Xe $3d$ photoionization.

The Doppler broadening Γ_D (in meV) was calculated from the equation [22]

$$\Gamma_D = 0.7215\sqrt{\frac{E_k T}{M}}, \tag{1}$$

where E_k, T, and M are the kinetic energy of the electron (in meV), temperature in K, and the mass of the target atom in amu, respectively.

The monochromator bandwidth was estimated by taking into account the vertical size of the photon beam, the surface errors of the mirrors, and the monochromator exit slit size in the calculations. At photon energy 64.10 eV, the calculated photon bandwidth with a 10-μm exit slit is 5.6 meV, which is in good agreement with He double-excitation absorbtion measurements done at the same energy on this beam line [26]. The nominal exit slit size of the monochromator was 10 μm during the measurements, but the actual slit size was not known accurately. At photon energies used for the Xe $4d$ photoelectron spectra (110–170 eV), the photon bandwidth is similar to the analyzer resolution. At photon energies used for Kr $3d$ photoionization (160–200 eV), the photon bandwidth is slightly bigger than the resolution of the analyzer, whereas in the Ar $2p$ measurements around 300 eV, the photon bandwidth dominates the total Gaussian contribution. It is thus essential to know accurately the photon-energy resolution used in the measurements. The Xe $3d$ photoelectron lines provided a means for this; at photon energies (730–780 eV) used for $3d$ ionization, the monochromator bandwidth almost completely determines the total Gaussian contribution. From the fit of nine $3d$ photoelectron spectra (see below), an average Gaussian contribution of 225 meV

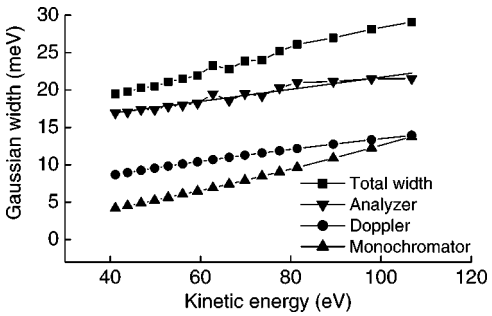

FIG. 2. The different experimental broadenings as a function of the kinetic energy as obtained from the analysis of the Kr $4p_{3/2}$ photoelectron spectra. The analyzer resolution was calculated by subtracting the monochromator bandwidth and Doppler broadening from the total linewidth of the Kr $4p_{3/2}$ photoelectron line. Analyzer resolution was fitted to follow the relation: $\Gamma_{analyzer}$ (meV) $=0.075\times E_{kin}$ (eV) $+13.8$ meV.

was obtained. Our calculated value with a 10-μm slit is 230 meV, in a very good agreement with the experimental result. Therefore we believe that our calculated values for the photon bandwidth are rather accurate.

After removing the monochromator and Doppler contributions from the total experimental linewidth, the analyzer contribution (calculated as $\sqrt{\Gamma_{tot}^2-\Gamma_{h\nu}^2-\Gamma_D^2}$) shows a linear behavior (see Fig. 2). With the constant pass energy of 10 eV, the analyzer contribution increases slightly from 17 to 21 meV over the initial kinetic energy range of 40–110 eV. This might be due to the effects of increased retardation on the focusing and angular-distribution properties of the electron lense on the analyzer.

IV. DATA ANALYSIS

When the ionization takes place above, but close to a core-ionization threshold, an asymmetric line shape usually occurs. This originates from the postcollision interaction (PCI) between the slow photoelectron and the subsequently emitted Auger electron in the vicinity of the electric field of the ion. In addition to the asymmetry in the line shape, also the apparent position of the electron line is affected. PCI may complicate the determination of the lifetime widths since it requires a specific line shape that depends on the model assumed. The Kr $3d$ and Xe $4d$ photoelectron spectra were measured only at such high-photon energies that PCI was of no concern, i.e., photoelectrons had larger kinetic energies than the Auger electrons. This was not purposeful in the measurements of Ar $2p$ and Xe $3d$ photoelectron spectra, since ionizations are in these cases followed by the emission of high kinetic energy Auger electrons.

The Ar $2p$, Kr $3d$, Xe $3d$, and $4d$ photoelectron lines were measured at several photon energies, keeping as many experimental variables the same as possible as in the calibration measurements using the Kr $4p_{3/2}$ photoelectron line, i.e., analyzer pass energy, gas pressure and monochromator exit slit size. The photoelectron lines were measured at the same kinetic energies as the Kr $4p_{3/2}$ line that enabled us to resolve the analyzer contribution very accurately. The low-pass mode of the analyzer voltage supplies was used to obtain the highest analyzer resolution with the used pass energy (10 eV) and analyzer slit settings (curved 0.5 mm). The drawback of using the high-accuracy voltage supplies was that the kinetic energy range was limited to the maximum value of 120 eV. This prevented us from measuring the Kr $4p$ photoelectron line for the photon-bandwidth calibration at the same photon energies as the studied core-photoelectron lines.

The photoelectron lines were analyzed using a least-squares fitting program [11]. The Lorentzian profile distorted by PCI is calculated using the formula given by Armen *et al.* [27]. The final line shape is obtained from the convolution of the inherent line shape (Lorentzian or PCI-disturbed Lorentzian) and the Gaussian shape. The important feature of the program is that up to ten different spectra can be fitted simultaneously while linking variables between separate spectra. This enabled us to link the lifetime widths for each subshell between the spectra. The Gaussian contribution was calculated from the analyzer, Doppler and photon broadenings for each kinetic energy and kept fixed during the fit. Every spectrum was first fitted individually to see possible changes in the lifetime widths. After this, variables between multiple spectra were linked and the fit was repeated.

Similar measurements, but with a shorter photon energy range were made during another beamtime to check the results of the first beamtime. During these measurements, the valence Ar $3p$, Kr $4p$ and Xe $5p$ photoelectron lines were measured at the same kinetic energies as the Ar $2p$, Kr $3d$ and Xe $4d$ core photoelectron lines, respectively. This time the photon bandwidth was determined by measuring the Ar $3p$ and Xe $5p$ photoelectron lines at the same few photon energies as used for Kr $3d$ and Xe $4d$ lines. Total ion yield measurements were performed using a time-of-flight spectrometer to evaluate the resolution of the beam line. The photon-energy resolution was this time slightly worse due to the storage-ring conditions, but the results for the lifetime widths were practically the same as from the spectra of first beam time.

V. RESULTS

A. Xe 4*d*

The Xe $4d$ photoelectron lines were measured at 16 different photon energies between 109–174 eV. The lowest kinetic energy of $4d_{3/2}$ photoelectrons was 40 eV, which is above the kinetic energies of all the $N_{4,5}OO$ Auger transitions. Thus a symmetric lineshape results, see Fig. 3. The upper limits for the Xe $4d_{3/2}^{-1}$ and $4d_{5/2}^{-1}$ lifetime widths are 107 and 114 meV, respectively, obtained by fitting the spectra with pure Lorentzian line shapes.

The results for the $4d^{-1}$ lifetime widths obtained from the spectra when fitted separately are shown in Fig. 4. The total experimental Gaussian contribution was calculated to vary from 22(2) to 33(2) meV at these kinetic energies. It was kept fixed in the fit, while the Lorentzian contribution was allowed to change freely. As we can see, the $4d_{5/2}^{-1}$ state has systematically a $\sim$7 meV higher lifetime width than the

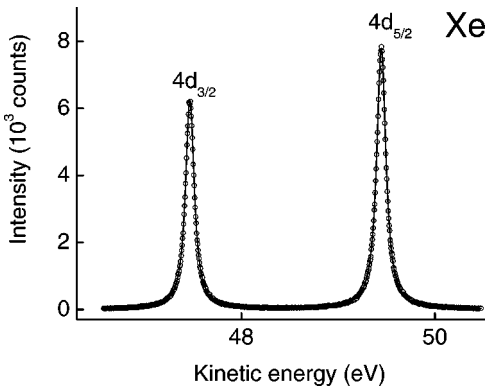

FIG. 3. Xe $4d$ photoelectron lines measured at 117.0-eV photon energy. The solid line shows the result of the least-square fit to the data points given by circles.

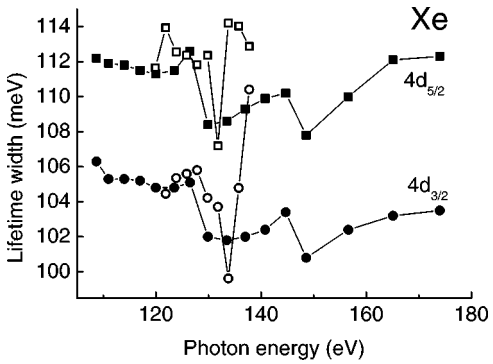

FIG. 4. Experimental lifetime widths of Xe $4d^{-1}$ states as a function of the photon energy as obtained by fitting the Xe $4d$ photoelectron lines individually. The open and filled symbols denote to measurements in the different beamtimes.

$4d_{3/2}^{-1}$ state. The photon energies overlap the Xe $4p^{-1}nl$ resonances at 140.8 and 144.7 eV, but there seems to be no conclusive effect on the $4d^{-1}$ lifetime widths. The variation of the values around the average originates most likely from the instrumental factors. Therefore, in the current photon energy range, we cannot verify the finding of Ausmees *et al.* [12] about the lifetime dependence on the photon energy.

Based on the assumption that the Xe $4d$ lifetime widths are constant in the current photon energy range, a new fit was performed by linking the lifetime widths of each line between separate spectra. When the calculated total Gaussian contributions were used in the fit, the lifetime widths of 104(3) and 111(3) meV were obtained for the $4d_{3/2}^{-1}$ and $4d_{5/2}^{-1}$ states, respectively. We believe that these values are quite accurate since the analyzer contribution clearly dominates the total Gaussian width and the absolute uncertainty in the estimated monochromator bandwidth is small. In addition, the Lorentzian widths are large compared to the Gaussian contribution.

The lifetime widths reported in the literature are compared with our results in Table I. The lifetime width of 110 meV for the $4d_{5/2}^{-1}$ state deduced from the $N_5O_{2,3}O_{2,3}$ ($^1S_0$) Auger line by Schmidt *et al.* [14] at 110-eV photon energy agrees very well with our measurements. Ausmees *et al.* [12] reported 110(2) and 118(2) meV for the $4d_{3/2}^{-1}$ and $4d_{5/2}^{-1}$ states at photon energy 109 eV. These values are 6–7 meV larger than our results.

In Table II we compare our results for the core-ionized states with those obtained for the resonantly excited states. King *et al.* [2] measured the lifetime widths of the Ar $2p^{-1}nl$, Kr $3d^{-1}nl$ and Xe $4d^{-1}nl$ states using electron energy loss technique. Their values of ~130 meV for the lifetime widths of the $4d^{-1}nl$ states are rather high. More recent values from Sairanen *et al.* [4] and from Masui *et al.* [5] agree better with our results.

B. Kr 3*d*

The Kr $3d$ photoelectron lines were measured at five different photon energies between 158–198 eV. At these energies the line shape is symmetric and not disturbed by the PCI, see Fig. 5. When both Lorentzian and Gaussian widths were free in the fit, a result of 91 meV was obtained for the $3d^{-1}$ lifetime width, but the Gaussian contribution became too low (~20 meV). We calculated that the correct Gaussian width should be 30(3) to 40(3) meV for this energy region in the present measurements. Using these values and linking the lifetime widths between spectra, we got an 88(4)-meV natural width for the Kr $3d$ levels. The fit gave only an 0.5 meV difference between the widths of the $3d$ spin-orbit

TABLE I. Experimental lifetime widths (meV) of the Ar $2p^{-1}$, Kr $3d^{-1}$, Xe $3d^{-1}$, and $4d^{-1}$ states compared with experimental values from the literature. The numbers in parenthesis show the error in the last significant digit. Numbers in square brackets refer to sources of literature from which values have been taken.

	This work				
Ar $2p_{1/2}$	118(4)	120 [8]		130(5) [10]	100(10) [11]
Ar $2p_{3/2}$	118(4)	120 [8]	120 [9]	130(5) [10]	107(10) [11]
Kr $3d_{3/2}$	88(4)				
Kr $3d_{5/2}$	88(4)				
Xe $4d_{3/2}$	104(3)	110(2) [12][a]	114(4) [13]		
Xe $4d_{5/2}$	111(3)	118(2) [12][a]	121(4) [13]	110 [14]	
Xe $3d_{3/2}$	490(30)	500 [15]	500 [16]		
Xe $3d_{5/2}$	510(30)	500 [15]	500 [16]		

[a]At photon energy 109 eV, error derived from the figure.

TABLE II. Lifetime widths for some of the Ar $2p^{-1}nl$, Kr $3d^{-1}nl$, and Xe $4d^{-1}nl$ resonantly excited states in comparison with the values obtained for the core-ionized states in this work. Not all resonant states are included in this table. The numbers in parenthesis show the error in the last significant digit. The numbers in square brackets refer to sources of literature where from values have been taken.

State				This work
Ar $2p_{3/2}^{-1}4s$	114(2) [4]	116(3) [3]	111(3) [6]	
$3d$	125(3) [4]		112(4) [6]	
$4d$	129(5) [4]		116(5) [6]	
$5d$	133(10) [4]			
$6d$	139(10) [4]			
$2p_{3/2}^{-1}$				118(4)
$2p_{1/2}^{-1}$ $4s$	109(3) [4]	118(4) [3]	111(3) [6]	
$6d$	133(10) [4]			
$2p_{1/2}^{-1}$				118(4)
Kr $3d_{5/2}^{-1}5p$	83(1) [4]	83(4) [2]		
$6p$	79(2) [4]			
$7p$	79(2) [4]			
$3d_{5/2}^{-1}$				88(4)
$3d_{3/2}^{-1}5p$	83(2) [4]			
$6p$	84(3) [4]	98(12) [2]		
$3d_{3/2}^{-1}$				88(4)
Xe $4d_{5/2}^{-1}6p$	109.8(1.0) [4]	111(4) [2]	106.3(0.5) [5]	
$7p$	109.1(1) [4]	128(9) [2]	106.0(0.5) [5]	
$8p$	103(3) [4]		104(1) [5]	
$9p$	98(8) [4]		104(2) [5]	
$4d_{5/2}^{-1}$				111(3)
$4d_{3/2}^{-1}6p$	107(1) [4]	119(8) [2]	104(1) [5]	
$7p$	106(3) [4]	133(15) [2]	106(5) [5]	
$9p$	104(5) [4]		106(3) [5]	
$4d_{3/2}^{-1}$				104(3)
Xe $3d_{5/2}^{-1}6p$	390(20) [7]			
$3d_{5/2}^{-1}7p$	450(20) [7]			
$3d_{5/2}^{-1}$				510(30)
$3d_{3/2}^{-1}$				490(30)

split components. This is well inside the error limits of our data analysis, and therefore we present only one lifetime width for the $3d^{-1}$ states.

The lifetime widths extracted from the Kr $3d$ photoelectron and Auger lines seem to be very rare in the literature; we could not find any. Therefore the comparison can only be made with the lifetime widths of the resonantly excited states. The natural widths of the Kr $3d^{-1}5p$ states are about 83 meV [2,4], and thus narrower than found in this work for the core-ionized states.

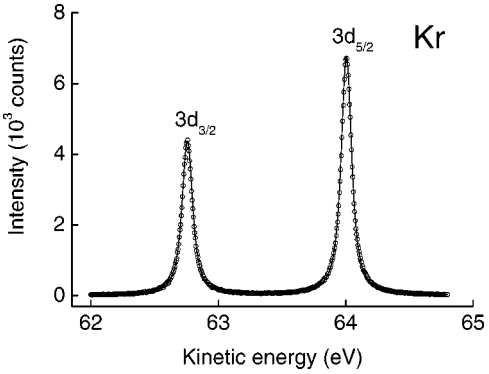

FIG. 5. Kr $3d$ photoelectron lines measured at 157.8-eV photon energy. The solid line shows the result of the least-square fit.

C. Ar $2p$

Ar $2p$ photoelectrons were measured at four photon energies between 289.5–304.8 eV. Because the $2p$ threshold is around 250 eV, the photoelectrons have lower kinetic energy than Auger electrons, which leads to a PCI-distorted line shape, see Fig. 6. At the kinetic energies of the measurements there are no main Auger lines and therefore the background is practically absent. The Gaussian width was calculated to be $\sim 60(5)$ meV at these energies from which the contribution of the photon bandwidth was ~ 56 meV. The fit with linked lifetime widths between the four spectra resulted in 1.3 meV higher lifetime width for the $2p_{3/2}^{-1}$ state than for the $2p_{1/2}^{-1}$ state. The difference is again inside the error limits of our data analysis; we present 118(4) meV as the lifetime widths for the $2p_{1/2}^{-1}$ and $2p_{3/2}^{-1}$ states.

Nordgren *et al.* [8] measured the Ar $2p^{-1}$ lifetime widths by means of x-ray emission technique and with 50-meV spectrometer resolution. Their value 120 meV agrees very well with our result. Recently, Carroll *et al.* [9] reported 120 meV for the $2p_{3/2}^{-1}$ lifetime width at 40 eV above the Ar $2p$ threshold, but found out that the fit of the experimental spectra gave higher values for the lifetime width close to the threshold. They explained that this may come from the insufficiency of the PCI model close to the threshold.

The value of 130(5) meV for the $2p$ lifetime width from Vikor *et al.* [10] is higher than other available results of

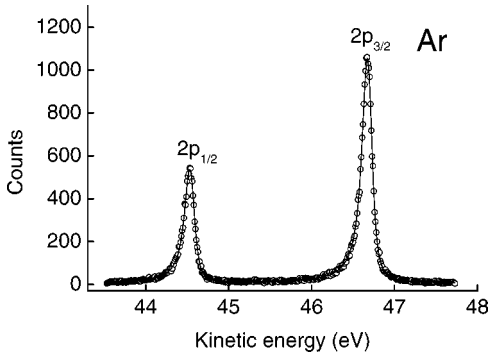

FIG. 6. Ar $2p$ photoelectron lines measured at 295.3-eV photon energy. The line shape is distorted by the PCI effect. The solid line shows the result of the least-square fit.

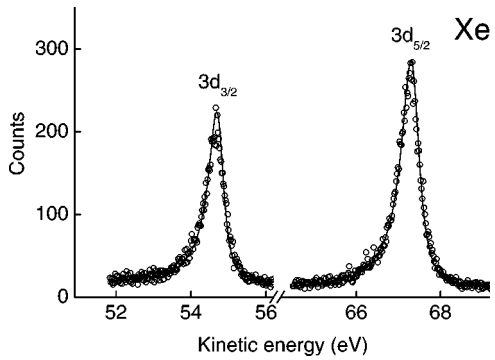

FIG. 7. Xe $3d$ photoelectron lines measured at 743.7-eV photon energy. The line shape is distorted by the PCI effect. The solid line shows the result of the least-square fit.

$\sim$120 meV. However, they pointed out that the discrepancy might be due to the less-well-understood PCI line shape in the presence of two electrons in the case of electron excitation. The lifetime widths of 100(10) and 107(10) meV for the $2p_{1/2}$ and $2p_{3/2}$ states were given by Köppe *et al.* [11]. These values are much lower than our results.

A very high resolution photoabsorption measurement of the Ar $2p \rightarrow nl$ excitations was performed by Prince *et al.* [6] at Elettra. Their results for the lifetime widths of the core-excited states are shown in Table II. They observe a slight increase in the lifetime width when going from the $2p_{3/2}^{-1}4s$ state [111(3) meV] to the $2p_{3/2}^{-1}4d$ state [116(5) meV]. The latter value approaches our result of 118(4) meV for the $2p_{3/2}^{-1}$ lifetime width. Unfortunately, they present the lifetime width only for the lowest $2p_{1/2}^{-1}nl$ state, so the comparison is left inadequate for the $2p_{1/2}^{-1}$ lifetime width.

D. Xe 3*d*

Nine photon energies between 731–784 eV were used to collect the Xe $3d$ photoelectron spectra. The intensity was low because the photon flux is reduced by two orders of magnitude at 750-eV photon energy compared to the maximum photon intensity at 130 eV on this beam line. However, we were able to collect enough statistics for a reliable data analysis by adding eight scans for each spectrum, see Fig. 7. The fit with all parameters free gave $\sim$225 meV for the average Gaussian width, which is close to our calculated value which varies from 210(30) to 240(30) meV in the current photon energy range. The fit using the calculated Gaussian contribution gave the lifetime widths of 490(30) meV and 510(30) meV for $3d_{3/2}^{-1}$ and $3d_{5/2}^{-1}$ states, respectively. The error limits are rather big and therefore it is not certain whether the lifetime widths really differ for the two $3d^{-1}$ states.

Svensson *et al.* [15] and Bancroft *et al.* [16] measured the Xe $3d$ photoelectron lines with monochromatized Al $K\alpha$ radiation. Their result of 0.5 eV for the $3d$ lifetime width is in good agreement with our data. The lifetime widths of Xe $3d_{5/2}^{-1}np$ $(n=6,7)$ states have been determined recently by Sankari *et al.* [7]. Their result is 390(20) meV for the $6p$ and 450(40) meV for the $7p$ resonance. The increasing tendency with n agrees with the larger lifetime width of the $3d_{5/2}^{-1}$ state.

VI. CONCLUSIONS

We have measured the Ar $2p$, Kr $3d$, Xe $3d$, and $4d$ photoelectron lines with very high resolution. From the experimental data we have obtained the lifetime widths of the core-ionized states with high accuracy. The previous literature values obtained from photoelectron or Auger studies agree reasonably well with our results, but our values are usually smaller. This may be due to the improved resolution in our measurements. The variation in the literature values for the lifetimes of the resonantly excited states is rather large, which complicates the comparison with our results. It appears, nevertheless, that the lifetime widths of the core-ionized and core-excited states are not quite the same. Absorption spectroscopy can be used to get an estimate for the lifetime width of the core-ionized state, but only through evaluation of the photoelectron spectrum one can obtain a reliable result. This, however, requires very high resolution, detailed knowledge on the widths and shapes of the contributing broadenings and if possible, such measurements that the line shapes are not disturbed by the PCI.

ACKNOWLEDGMENTS

We wish to thank V. Pennanen, M. Huttula, and E. Kukk for the help during the measurements and Professor H. Aksela for the critical reading of the manuscript. The assistance of the Maxlab staff is also acknowledged. This work has been supported by the Finnish Academy for the Natural Sciences, National Graduate School in Materials Physics (NGSMP), and by the European Community—Access to Research Infrastructure action of the Improving Human Potential Programme.

[1] V. Schmidt, *Electron Spectrometry of Atoms Using Synchrotron Radiation* (Cambridge University Press, Cambridge, 1997).

[2] G.C. King, M. Tronc, F.H. Read, and R.C. Bradford, J. Phys. B **10**, 2479 (1977).

[3] D.A. Shaw, G.C. King, F.H. Read, and D. Cvejanović, J. Phys. B **15**, 1785 (1982).

[4] O.-P. Sairanen, A. Kivimäki, E. Nõmmiste, H. Aksela, and S. Aksela, Phys. Rev. A **54**, 2834 (1996).

[5] S. Masui, E. Shigemasa, A. Yagishita, and I.A. Sellin, J. Phys. B **28**, 4529 (1995).

[6] K.C. Prince, M. Vondráček, J. Karvonen, M. Coreno, R. Camilloni, L. Avaldi, and M. de Simone, J. Electron Spectrosc. Relat. Phenom. **101-103**, 141 (1999).

[7] R. Sankari, A. Kivimäki, M. Huttula, H. Aksela, S. Aksela, M. Coreno, G. Turri, R. Camilloni, M. de Simone, and K.C.

Prince, Phys. Rev. A **63**, 032715 (2001).
[8] J. Nordgren, H. Ågren, C. Nordling, and K. Siegbahn, Phys. Scr. **19**, 5 (1979).
[9] T.X. Carroll, J. Hahne, T.D. Thomas, L.J. Sæthre, N. Berrah, J. Bozek, and E. Kukk, Phys. Rev. A **61**, 042503 (2000).
[10] Gy. Víkor, L. Tóth, S. Ricz, Á. Kövér, J. Végh, and B. Sulik, J. Electron Spectrosc. Relat. Phenom. **83**, 235 (1997).
[11] H.M. Köppe, A.L.D. Kilcoyne, J. Feldhaus, and A.M. Bradshaw, J. Electron Spectrosc. Relat. Phenom. **75**, 97 (1995).
[12] A. Ausmees, A. Hahlin, S.L. Sorensen, S. Sundin, I. Hjelte, O. Björneholm, and S. Svensson, J. Phys. B **32**, L197 (1999).
[13] A. Ausmees, S.J. Osborne, R. Moberg, S. Svensson, S. Aksela, O.-P. Sairanen, A. Kivimäki, A. Naves de Brito, E. Nõmmiste, J. Jauhiainen, and H. Aksela, Phys. Rev. A **51**, 855 (1995).
[14] V. Schmidt, S. Krummacher, F. Wuilleumier, and P. Dhez, Phys. Rev. A **24**, 1803 (1981).
[15] S. Svensson, N. Mårtensson, E. Basilier, P.Å. Malmquist, U. Gelius, and K. Siegbahn, Phys. Scr. **14**, 141 (1976).
[16] G.M. Bancroft, P.-Å. Malmqvist, S. Svensson, E. Basilier, U. Gelius, and K. Siegbahn, Inorg. Chem. **17**, 1595 (1978).
[17] M. Bässler, J.-O. Forsell, O. Björneholm, R. Feifel, M. Jurvansuu, S. Aksela, S. Sundin, S.L. Sorensen, R. Nyholm, A. Ausmees, and S. Svensson, J. Electron Spectrosc. Relat. Phenom. **101-103**, 953 (1999).
[18] R. Nyholm, S. Svensson, J. Nordgren, and A. Flodström, Nucl. Instrum. Methods Phys. Res. A **246**, 267 (1986).
[19] S. Aksela, A. Kivimäki, R. Nyholm, and S. Svensson, Rev. Sci. Instrum. **63**, 1252 (1992).
[20] S. Svensson, J.-O. Forsell, H. Siegbahn, A. Ausmees, G. Bray, S. Södergren, S. Sundin, S.J. Osborne, S. Aksela, E. Nõmmiste, J. Jauhiainen, M. Jurvansuu, J. Karvonen, P. Barta, W.R. Salaneck, A. Evaldsson, M. Lögdlund, and A. Fahlman, Rev. Sci. Instrum. **67**, 2149 (1996).
[21] N. Mårtensson, P. Baltzer, P.A. Brühwiler, J.-O. Forsell, A. Nilsson, A. Stenborg, and B. Wannberg, J. Electron Spectrosc. Relat. Phenom. **70**, 117 (1994).
[22] P. Baltzer, L. Karlsson, M. Lundqvist, and B. Wannberg, Rev. Sci. Instrum. **64**, 2179 (1993).
[23] K. Siegbahn, C. Nordling, G. Johansson, J. Hedman, P.F. Hedén, K. Hamrin, U. Gelius, T. Bergmark, L.O. Werme, R. Manne, and Y. Baer, *ESCA Applied to Free Molecules* (North-Holland, Amsterdam, 1969).
[24] A. Kivimäki, S. Heinäsmäki, M. Jurvansuu, S. Alitalo, E. Nõmmiste, H. Aksela, and S. Aksela, J. Electron Spectrosc. Relat. Phenom. **114-116**, 49 (2001).
[25] H. Petersen, Nucl. Instrum. Methods Phys. Res. A **246**, 260 (1986).
[26] Margit Bässler (private communication).
[27] G.B. Armen, J. Tulkki, T. Åberg, and B. Crasemann, Phys. Rev. A **36**, 5606 (1987).